# 埋弧焊烧结焊剂中 MnO 应用的试验分析

李继红, 刘 斌, 张 敏
(西安理工大学 材料科学与工程学院, 西安 710048)

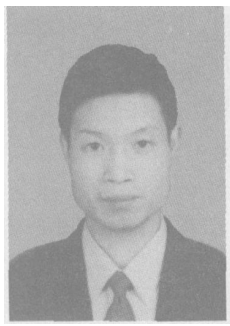

李继红

摘 要: 通过对烧结焊剂中常用组分 MnO 的物理化学性质的分析, 试制了三种烧结焊剂, 并进行了接头组织及力学性能的对比试验。结果表明, 烧结焊剂中加入适量的 MnO, 对提高焊剂的碱度、增加焊剂还原性、净化焊缝、改善脱渣、成形等工艺性能具有很大的作用。与此同时, 适量 MnO 的加入, 还可以合理控制焊缝金属中 Mn 的含量, 稳定奥氏体, 降低 $\gamma\rightarrow\alpha$ 转变温度, 为焊接接头组织中针状铁素体的形成创造良好的环境, 并进一步提高了焊缝金属的力学性能。

关键词: 烧结焊剂; MnO; 韧度; 工艺性能
中图分类号: TG113 文献标识码: A 文章编号: 0253－360X(2007)03－033－03

## 0 序 言

烧结焊剂作为一种新型的焊接材料, 从 20 世纪 80 年代引入国内以来, 广泛应用于锅炉、压力容器、化工容器、核电站、桥梁、船舶和焊管等重要的钢结构制作和连接中[1]。

与以前使用的熔炼焊剂相比较, 烧结焊剂具有制造过程耗能小、无污染、易机械化和自动化生产的特点。与此同时, 应用烧结焊剂埋弧焊方法所得到的焊接接头, 其焊缝金属合金化的效果好, 接头的力学性能能够得到有效的保证, 因而成为埋弧焊接过程中主要焊接材料之一。

目前高韧度烧结焊剂主要采用氟碱型渣系。其中 MnO 作为焊剂中增强增韧的一种主要组分, 在高韧度钢材烧结焊剂的成分配比中占有很大比例。文中从 MnO 的物理化学性能分析入手, 通过不同 MnO 含量烧结焊剂所施焊得到的焊缝金属的工艺性能、组织及力学性能的测试对比, 进一步分析 MnO 成分对焊接接头成形工艺及接头力学性能的影响规律。

## 1 MnO 对焊剂碱度的影响

碱度是描述焊剂性能的最主要的指标之一, 埋弧焊焊缝中的扩散[H] 含量、[O] 含量、力学性能等均与碱度有关。焊剂的碱度可按国际焊接学会(IIW)推荐的公式计算[2], 即

$$B_{\mathrm{IIW}}=\frac{\mathrm{CaO}+\mathrm{MgO}+\mathrm{BaO}+\mathrm{Na_2O}+\mathrm{K_2O}+\mathrm{CaF_2}+0.5(\mathrm{MnO}+\mathrm{FeO})}{\mathrm{SiO_2}+0.5(\mathrm{Al_2O_3}+\mathrm{Ti_2O_3}+\mathrm{ZrO_2})}, \tag{1}$$

式中: $B_{\mathrm{IIW}}$ 为烧结焊剂的碱度; 各化学式分别代表各化学物质在烧结焊剂中的质量分数。从式(1)中可以看出 MnO 的加入, 能提升烧结焊剂的碱度, 增加烧结焊剂的还原性, 净化焊缝金属。而且在氟碱型烧结焊剂中, MnO 不仅可以像 $SiO_2$ 那样降低熔渣熔点, 改善熔渣流动性, 而且可以降低表面张力, 有利于焊缝成形。

Harrison 等人[3] 认为, 在通常的焊缝金属冷却速度(800～500 ℃, 3～30 ℃/s)时, Mn 会抑制奥氏体向珠光体的转变, 为针状铁素体的形成创造条件, 从而改善焊缝金属的力学性能。从组织来看, 材料在冷却凝固过程中, 其奥氏体转变温度有以下的预测公式[4], 即

$$T_{\mathrm{sta}}=A_{C3}=910-203\sqrt{\mathrm{C}}-30\mathrm{Mn}-152\mathrm{Ni}+44.7\mathrm{Si}+104\mathrm{V}+31.5\mathrm{Mo}+400\mathrm{Ti}, \tag{2}$$

式中: $T_{\mathrm{sta}}$ 为奥氏体转变温度; 各元素符号表示各物质在焊缝中的质量分数。如果 $T_{\mathrm{sta}}$ 较低(＜853 K), 则认为不发生先共析铁素体的转变。从式(2)中可以看出, 烧结焊剂中 Mn 元素的含量对焊缝组织冷

收稿日期: 2006－12－04
基金项目: 陕西省教育厅科研计划项目(05JK277)

却及成形过程中组织的转变有很大的影响。

## 2 MnO 对接头成形工艺的影响

### 2.1 试验材料及焊接工艺

文献[5]指出，烧结焊剂熔点应低于被焊金属熔点200 ℃左右，熔化温度区间以 50 ~ 150 ℃为好。为了研究烧结焊剂中 MnO 的含量对工艺性能的影响，试制了不同 MnO 含量的烧结焊剂(编号为 1 号，2 号和3 号)，其主要组分见表 1。

表 1 试验焊剂的主要组分(质量分数，%)

Table 1 Compositions of experimental fluxes

| 序号 | $CaF_2$ | MgO | $Al_2O_3$ | MnO | $TiO_2$ | $SiO_2$ | $B_2O_3$ | Re(Mg) | 其它 |
|---|---|---|---|---|---|---|---|---|---|
| 1 | 20.3 | 25.8 | 12.0 | — | 5.1 | 20.6 | 1.7 | 0.2 | 3 ~ 7 |
| 2 | 20.0 | 24.0 | 13.1 | 8.1 | 8.0 | 18.6 | 1.9 | — | 3 ~ 7 |
| 3 | 20.7 | 21.5 | 11.3 | 16.1 | 7.6 | 18.2 | 2.1 | — | 3 ~ 7 |

焊接材料为研制的烧结焊剂，匹配焊丝选用管线钢用焊丝 H08C，试验用钢板为 X80 管线钢，厚度为7.9 mm，采用不开坡口双面焊接，正面焊完后反面清根焊接，钢板化学成分见表 2。焊接时的工艺参数为电流 520 ~530 A，电压 30 ~ 32 V，焊接速度 26 m/h。

表 2 X80 管线钢的化学成分(质量分数，%)

Table 2 Chemical compositions of X80 pipeline steel

| C | Si | Mn | Nb | V | Cu | Ni | Mo | S | P |
|---|---|---|---|---|---|---|---|---|---|
| 0.06 | 0.24 | 1.57 | 0.04 | 0.01 | 0.045 | 0.14 | 0.29 | 0.005 | 0.033 |

### 2.2 试验结果及分析

试验所得烧结焊剂工艺性能评定见表 3。

表 3 试验焊剂工艺性能评定

Table 3 Technic assessment of experimental fluxes

| 工艺评定 | 1 号 | 2 号 | 3 号 |
|---|---|---|---|
| 碱度 | 1.6 | 1.75 | 1.82 |
| 成形效果 | 75 | 80 | 85 |
| 脱渣效果 | 75 | 80 | 85 |

注：工艺评定标准为优 (90 分以上)、良(79 ~ 89 分)、中(60 ~ 79 分)、差(60 分以下)

从表 3 中可以看出，按照 1 号，2 号和 3 号的排列顺序，焊缝金属脱渣和成形效果依次升高。高韧度氟碱型烧结焊剂的研制，势必会加入还原性较高的碱性氧化物，其熔点一般都很高，例如：MgO (2 800 ℃)，$Al_2O_3$(2 050 ℃)，$ZrO_2$ (2 715 ℃)。这些弱氧化性的物质的加入，虽然能提高焊缝金属的纯净度，改善焊缝金属力学性能；但是另一方面高熔点物质的加入对熔渣流动性、表面张力以及成形都有很大的负面影响。MnO 的熔点为1 650 ℃，比较接近钢的熔点，能很好地协调烧结焊剂熔点，改善焊接工艺性能。因此，随烧结焊剂中 MnO 的增多，其工艺性能会得到改善。

## 3 MnO 对焊缝金属力学性能的影响

试验采用 H08C 与试制焊剂进行匹配，对 X80 钢板进行焊接，焊接工艺同上，所得焊缝金属化学成分见表 4。采用 Neopht—21 型卧式金相显微镜观察焊缝金属显微组织如图 1 所示。

表 4 试验焊剂焊缝金属主要化学成分(质量分数，%)

Table 4 Chemical compositions of deposited metals using experimental fluxes

| 序号 | C | Mn | Si | Mo | Ti | B | S | P |
|---|---|---|---|---|---|---|---|---|
| 1 | 0.06 | 1.04 | 0.24 | 0.023 | 0.020 | 0.001 | 0.008 | 0.013 |
| 2 | 0.06 | 1.68 | 0.22 | 0.020 | 0.018 | 0.001 | 0.012 | 0.018 |
| 3 | 0.07 | 1.95 | 0.27 | 0.025 | 0.017 | 0.001 | 0.011 | 0.017 |

从图 1 中可以看出，3 种烧结焊剂所得焊缝金属都含有不同程度的针状铁素体组织(AF)。图 1b 中 2 号焊剂所得焊缝金属组织 90%都是由针状铁素体组成，其针状铁素体的含量比图 1a 中 1 号和图 1c中3 号焊剂的含量要多，形态分布上表现为彼此咬合、互相交错分布。1 号烧结焊剂所得焊缝金属含有较多的先共析铁素体组织，3 号烧结焊剂所得焊缝金属更多地表现为贝氏体组织。为了进一步分析焊剂中 MnO 对焊缝金属力学性能的影响，分别对 1 号，2 号和 3 号焊剂焊缝金属在 JB —30B 冲击试验机上进行了冲击韧度试验，在 PCS —25T 拉伸试验机上进行拉伸试验，所得力学性能见表5。

表 5 焊缝金属力学性能

Table 5 Mechanical properties of deposited metals using experiment fluxes

| 序号 | 屈服强度 $R_{eL}$/MPa | 抗拉强度 $R_m$/MPa | 断后伸长率 $A$(%) | 断面收缩率 $Z$(%) | 冲击吸收功 $A_{kV}$/J −20 ℃ | 冲击吸收功 $A_{kV}$/J −40 ℃ |
|---|---|---|---|---|---|---|
| 1 | 534 | 631 | 24.2 | 55.47 | 128 | 110 |
| 2 | 557 | 681 | 24.2 | 55.47 | 186 | 162 |
| 3 | 572 | 662 | 21.6 | 56.76 | 167 | 103 |

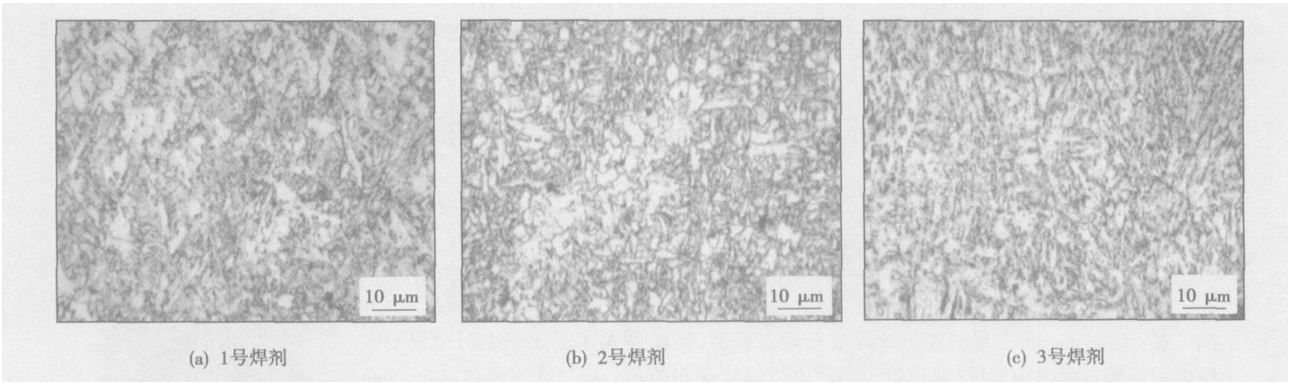


图 1　试制焊剂焊缝金属显微组织

Fig. 1　Optical microscopy of weld

从表 5 中可以看到，2 号焊剂所得焊缝金属的低温冲击韧度比 1 号和 3 号焊剂所得焊缝金属冲击韧度都要好，且具有较高的屈服强度。3 号焊剂的屈服强度比 1 号焊剂要高，但是其冲击韧度要稍低于 1 号焊剂。结合焊缝金属化学成分（表 4）及显微组织（图 1）分析得知，由 1 号烧结焊剂埋弧焊所得到的焊缝金属由于较少的 Mn 含量，$\gamma \rightarrow \alpha$ 转变在较高温度下形成先共析铁素体比较多。而与此相反的是，3 号烧结焊剂埋弧焊接所得到的焊缝金属中由于含有过多 Mn，$\gamma$ 变得异常稳定，在冷却过程中不能及时析出针状铁素体，从而在较低的温度下形成贝氏体组织。针状铁素体是中温相变产物，其本质是晶内形核的贝氏体，形成温度范围为 600 ~ 500 ℃。晶粒细小，其宽度一般为 1 ~ 3 μm，长宽比约为 3∶1 ~ 10∶1，相邻针状铁素体间的方位差为大倾角，并以大角度分布，一般在 20° 以上，取向自由度大，裂纹不容易扩展，具有良好的强韧性特征[6,7]。贝氏体强度优于先共析铁素体，但是韧性却不及之，故表现为 2 号焊剂性能最好，3 号烧结焊剂所得焊缝金属强度高于 1 号焊剂，而韧性较 1 号焊剂有所降低。

## 4　结　　论

（1）烧结焊剂中 MnO 的加入能提高焊剂碱度，提高焊缝纯净度。改善渣的流动性、表面张力以及成形效果，能很好地改善碱性烧结焊剂工艺性能。

（2）Mn 是奥氏体稳定元素，合理加入能为针状铁素体的形成创造良好条件，提高焊缝金属力学性能。2 号焊剂匹配 H08C 焊丝所得焊缝金属 Mn 含量约在 1.7% 左右，获得较高的屈服强度和良好的冲击韧度。

## 参考文献：

[1] 马彩玲，何少卿. 烧结焊剂的应用及其发展趋势[J]. 电焊机，2006，36(4)：10－14.

[2] 苏仲鸣. 焊剂的性能与使用[M]. 北京：机械工业出版社，1989.

[3] Farrar R A，Harrison P L. Acicular ferrite in carbon-manganese weld metals：an overview [J]. J. Mater Set，1987，22(12)：3812－3820.

[4] 张国栋，李志远，余圣甫. 药芯焊丝焊缝中先共析铁素体的数量预测[J]. 电焊机，2001，31(11)：17－20.

[5] Davis M L E，Bailey N. Properties of submerged arcfluxes-a foudmental study[J]. Metal Construction，1982(3)：202－209.

[6] Sugden A B B，Bhadeshia H K D H. Lower acicular ferrite[J]. Metallurgical Ransaction A，1989，20(9)：1811－1818.

[7] Babu S S，Bhadeshia H K D H. Mechanism of the transition from bainite to acicular ferrite[J]. Materials Transaction，1991，32(2)：679－688.

作者简介：李继红，男，1973 年出生，博士。主要从事新型焊接材料、焊接结构断裂强度及焊接工程结构方面的研究工作，发表论文 10 余篇。

Email：lijihong@xaut.edu.cn

China; 2. School of Applied Science, Beijing University of Science and Technology, Beijing 100083, China; 3. The Power Institute of Hebei Province, Shijiazhuang 050021, China). p17—20

**Abstract**: The microstructure and micro-hardness have been studied on the T91/G102 dissimilar steel welded joints before and after a long-time run. The results showed that the long-time run had little effect on the T91 HAZ microstructure, but had a definite effect on weld and the G102 HAZ microstructure. After the long-time run, the fine particle bainite in the welding normalized zone kept its fine microstructure and at the same time precipitated lots of fine chip-like carbides, which was proved to be $M_6C$ carbide by TEM analyses. The lath bainite in the original matrix was transformed into tempered bainite without remaining any lath feature and precipitated lots of the block ferrite grains and chain-shape carbides instead. The results also showed that the micro-hardness on the T91 HAZ almost kept the same after its long-time run and the micro-hardness on the weld and G102 matrix dropped down. However, the micro-hardness in the heat affect zone of G102 went up unexpectedly.

**Key words**: dissimilar steel; welded joint; micro-hardness

**Fabrication of mono-layer diamond drill bit by brazing and its microstructure on the interfaces** ZHANG Fenglin, ZHOU Yumei, WANG Chengyong (Faculty of Mechanical and Electronic Engineering, Guangdong University of Technology, Guangzhou 510006, China). p21—24

**Abstract**: Mono-layer diamond drill bit was fabricated by high temperature brazing. The performance of brazed drill bit was compared with the electro-plated diamond drill bit in the hole drilling of silicate glass. It was found that the sharpness and the tool life of the brazed drill bit are superior to the electro-plated one due to the higher diamond grit protrusion and cohesion between diamond and filler alloy. By observation of optical microscope, scanning electron microscope, energy dispersive X-ray analysis and X-ray diffraction analysis, the microstructure and the composition of the interfaces on steel substrate-filler alloy-diamond were investigated. The diffusion of Ni and Cr from filler alloy into steel substrate was found. Reaction layers in filler alloy and diamond were identified respectively. Main phases in filler alloy reaction layer are $Cr_3C_2$ and $Cr_7C_3$, which are the reaction products of the diffusion carbon and Cr in the filler alloy. The reaction layer in diamond may be induced by the penetration of Cr into the dislocation core of graphitized diamond and formation of $Cr_3C_2$.

**Key words**: brazing; diamond drill bit; interface; microstructure

**$CO_2$ laser welding of tailored 5A02 aluminum alloy sheets with different thickness using filler powder** YU Shurong[1], FAN Ding[1], XIONG Jinhui[2], WANG Gang[2], CHEN Jianhong[2] (1. State Key Laboratory of Gansu Advanced Non-ferrous Metal Materials, Lanzhou University of Technology, Lanzhou 730050, China; 2. Key Laboratory of Non-ferrous Metal Alloys, The Ministry of Education, Lanzhou University of Technology, Lanzhou 730050, China). p25—28

**Abstract**: $CO_2$ laser was used to weld 5A02 aluminum alloys sheet with different thickness with filler metal powder and without powder. The influences of the filler metal powder on the weld appearance and process stability was studied. Using tensile tests, microscope and SEM, the mechanical and microstructure characteristics of the welded joints were evaluated, and the effect of the weld distribution on the plastic formability of the TWB (tailored welded blanks) were analyzed. The results indicate that the addition of the metal powder can enhance the energy coupling efficiency during laser welding of 5A02 aluminum alloys sheet with different thickness, and the weld appearance and process stability can be improved greatly. In a wide range of parameters for this alloy sheet with different thickness, the weld appearance is very well. The total elongation in the longitudinal direction for the laser welds decreased greatly. The specimens of the TWB in the transverse direction all fractured on the HAZ of the thinner base metal, the main reason is the thinner base metal of half-harded state was annealed during welding. The ductibility of the TWB is effected by percent of the sheet in a TWB. The total elongation increases with the percent of the sheet with better ductibility. The microstructure of the welds from the fusion line to the weld is cellular dendrite structure, and it is the finer equl-axed grains in the center of fusion zone.

**Key words**: $CO_2$ laser welding; tailor welded blank; aluminum alloy; different thickness

**Characteristics of dynamic welding angular distortion of an aluminum alloy with TIG welding** WANG Rui, LIANG Zhenxin, ZHANG Jianxun (School of Material Science and Engineering, Xi'an Jiaotong University, Xi'an 710049, China). p29—32

**Abstract**: The characteristics of dynamic welding angular distortions of aluminum alloy 5A12 with TIG welding are investigated by self-made welding dynamic temperature and distortion measuring system. With analyzing the welding thermal cycle and dynamic angular distortion curves, two characteristic values, the down warping maximum point and warping balanced point are put forward to describe the dynamic curve behavior. The changing rules of the dynamic curves under different welding parameters are investigated by means of orthogonal experiment method. Based on the results, mathematic model on the dynamic angular distortion curve is introduced. The results show the dynamic angular distortion can be expressed by the mathematic formula accurately. The down warping maximum point, warping balanced point and the slops of the curves are the key factors that characterize the dynamic angular distortion curves.

**Key words**: aluminum alloy; dynamic deformation; dynamic characteristic values; mathematic model

**Application of MnO for submerged arc agglomerated flux** LI Jihong, LIU Bin, ZHANG Min (School of Materials Science and Engineering, Xi'an University of Technolog, Xi'an 710048, Chi-

na). p33—35

**Abstract**: According to the physical and chemical properties of the common composition of agglomerated flux-MnO, three kinds of agglomerated flux were prepared and the parallel tests on weld microstiuctures and the mechanical property were discussed also. The result shows that the addition of MnO in the agglomerated flux not only incneases the alkalinity of the flux and its reducibility, and purifies the weld, and improves the slag detachability and the formation ability and processing abilities, but also can stabilize the austenite, and reduce the $\gamma \rightarrow \alpha$ transformation temperature by controlling the quantity of Mn in the weld metal when MnO is added in, which will make a good environment for the formation of the acicular ferrite and the promotion of the mechanical property of the weld metal.

**Key words**: agglomerated flux; MnO; toughness; processing property

**Simulation of multiphase transient fluid flow field and temperature field during plasma powder multi-layer deposition process** ZENG Lingfang, WANG Guilan, ZHANG Haiou, KONG Fanrong (Huazhong University of Science and Technology, Wuhan 430074, China). p36—40

**Abstract**: A 2D transient mathematical model was developed to investigate plasma powder deposition shaping process, presenting the free surface evolution of multilayer and the simulation of fluid flow and heat transfer. The Level-Set approach was adopted to deal with some factors such as deposited track, liquid/vapor interface, which considered surface tension gradient (the major driving forces for the melt flow), interface curvatures, buoyancy and convection heat loss. The SIMPLEC algorithm was used for solving the governing equations. The results obtained by the simulation were in agreement with those measured in experiment, and the effect of the deposition process parameters such as input current, scanning velocity and powder feeding rate on the profile of deposition layer and shaping quality was analyzed.

**Key words**: plasma deposition; Level-Set approach; SIMPLEC algorithm

**Effect of thermal cycles on interface evolution of vacuum diffusion bonded aluminum alloy 2A14** LI Jinglong, XIONG Jiangtao, ZHANG Fusheng (Shanxi Key Laboratory of Friction Welding Technologies, Northwestern Polytechnical University, Xi'an 710072, China). p41—44

**Abstract**: Wrought aluminum alloy 2A14 samples were diffusion bonded at 500 ℃, 530 ℃ and 560 ℃ respectively for 60 min under the bonding pressure of 4 MPa and a vacuum pressure lower than $3.4 \times 10^{-3}$ Pa. The bonding ratio, the morphologies of the interface and the microstructures of the base metal were examined by scanning electron microscope. The results showed that at 500 ℃ lower than the solid solution line, the interface after welding remained straight as original in which only a little metallurgical bonding points were presented leading to a very low bonding ratio. At 530 ℃ above the solid solution line but below the Al-Cu eutectic point, $CuAl_2$ phase joining additionally contributed to the bonding mechanism hence the bonding ratio increased apparently. When the temperature was further raised to 560 ℃ above the eutectic point, $CuAl_2$ phase dissolved and the eutectic liquid formed at the crystal boundaries. The liquid was then extruded into the interface which crashed the oxidation film and filled the interface voids so that the bonding ratio increased remarkably. Therefore, a wavy bonded interface, composed of crystal boundaries, substituted the original straight interface. Based on the analyses, a model was proposed for liquid phase formation at the crystal boundaries and oxidation film crash.

**Key words**: diffusion bonding; 2A14 aluminum alloy; eutectic temperature; bonding ratio

**Microstructure and strength of $Si_3N_4$ joint brazed with Ti40Zr25Ni15Cu20 amorphous brazing alloy** ZOU Jiasheng, ZHAO Hongquan, JIANG Zhiguo (Provincial Key Laboratory of Advanced Welding Technology, Jiangsu University of Science and Technology, Zhenjiang 212003, Jiangsu, China). p45—48

**Abstract**: $Si_3N_4$ ceramic is brazed with Ti40Zr25Ni15Cu20 amorphous filler metal, and the effect of brazing parameter on interfacial microstructure and joint strength was discussed. The interfacial microstructure is composed of two parts which are TiN and Ti-Si, Zr-Si compound respectively with the SEM, EDX etc. Under the same experiments conditions, the joint strength brazed with amorphous filler metal increased a lot compared with the crystalline.

**Key words**: Ti-Zr-Ni-Cu brazing filler metal; amorphous filler metal; $Si_3N_4$ ceramic; interfacial microstructure; bonding strength

**Partial least square approach for multi-parameter assessment of resistance spot welding quality** LI Ruihua[1], MENG Guoxiang[1], GONG Liang[1], ZHANG Ke[2] (1. School of Mechanical Engineering, Shanghai Jiaotong University, Shanghai 200240, China; 2. Institute of Weld Engineering, Shanghai Jiaotong University, Shanghai 200240, China). p49—52

**Abstract**: A new approach based on partial least square (PLS) was used in the multi-parameter monitoring and analysis of the resistance spot welding (RSW) quality. Based on the idea of extracting principal components, correlation information between the monitored RSW parameters and welding quality were screened and synthesized under the condition that the multi-parameters monitored exist multicollinearity. Moreover, various data message of the RSW quality process parameters were also shown and discussed. In addition, an integrated assessment model was built based on multi-parameter monitored. The experimental results indicate that the presented method can select and extract PLS components of RSW quality process parameters from sample data, and the problems of high dimension and multicollinearity are solved effectively in regression model. The integrated evaluation model has excellent estimation ability.

**Key words**: resistance spot welding; quality model; multi-